http://dx.doi.org/10.5935/0103-5053.20150274

J. Braz. Chem. Soc., Vol. 27, No. 2, 349-362, 2016.
Printed in Brazil - ©2016 Sociedade Brasileira de Química
0103 - 5053 $6.00+0.00

Article

Self-Organization in Ionic Liquids: From Bulk to Interfaces and Films

Karina Shimizu,*[*,a,b] Mohammad Tariq,[#,b] Adilson A. Freitas,[a] Agílio A. H. Pádua[c] and José N. C. Lopes*[*,a,b]

[a]*Centro de Química Estrutural, Instituto Superior Técnico, Universidade de Lisboa, 1049-001 Lisbon, Portugal*

[b]*Instituto de Tecnologia Química e Biológica, Universidade Nova de Lisboa, 2780-157 Oeiras, Portugal*

[c]*Laboratoire Thermodynamique et Interactions Moléculaires, CNRS/Université Blaise Pascal, Clermont-Ferrand, France*

In this contribution we present an overview on the relation between the complex structure of ionic liquids (ILs) and its impact in the field of surface science. The results herein described result mainly from modeling and simulation work carried out at Centro de Química Estrutural, Universidade de Lisboa, complemented in some cases by experimental results obtained at Instituto de Tecnologia Química e Biológica, Universidade Nova de Lisboa or elsewhere. The overview starts with the description of nano-segregation and self-aggregation phenomena experienced by pure ionic liquids in bulk phases (bi-continuous structures in the isotropic liquid or the formation of liquid-crystal phases). This is followed by the analysis of IL self-aggregation in molecular solvent solutions (micelle or gel formation). The second part of the overview is devoted to the study of the structuration of ILs at the IL/vacuum, IL/liquid or IL/solid interfaces. The final part deals with thin IL films stabilized between air/solid, air/liquid or solid/solid boundaries.

Keywords: molecular dynamics, nano-segregation, micelle, structure factor, nanostructured fluid

Introduction

Ionic liquids (ILs) are a new class of salts with unusually low melting point temperatures (100 ºC is the commonly accepted upper limit). Since their introduction in the last decade of the 20th century, there has been an enormous interest from the academic and industrial communities that resulted on a vast amount of fundamental and applied research work. Many industrial applications are currently being developed or are already implemented.[1] ILs are considered potential substitutes for traditional solvents due to a unique set of properties such as negligible vapor pressure, high thermal stability, non-flammability, wide electrochemical window, enhanced solvent quality and easy recycling.

Despite the recent widespread use of ILs for different types of application, including many where interfaces play a central role, they have not yet been fully subjected to the same level of molecular scrutiny experienced by more traditional surfaces or interfaces.[2-6] For instance, ILs are finding use as gas-capture media. This process involves collisions between gas-phase molecules and the IL surface, which is an important mass transfer step leading to equilibrium. This elementary process is highly dependent on the chemical/structural nature of the liquid surface.[7]

Ionic liquids are salts, substances composed essentially of cations and anions. This fact differentiates them from simple ionic solutions, where ions are dissolved in a molecular medium. The lack of a molecular solvent has a profound impact in the structure of the ionic fluid near a surface boundary. This overview encompasses our most recent efforts in the investigation of such behavior.

Figure 1 depicts diagrammatically the layout of the present work: the first two sub-sections of the Results and Discussion section deal with the nano-segregated or self-organized structures of ILs in bulk phases, either as pure substances (Figures 1a and 1b), or in mixtures

*e-mail: karina.shimizu@tecnico.ulisboa.pt, jnlopes@tecnico.ulisboa.pt
#Present address: Department of Chemical Engineering, College of Engineering, Qatar University, 2713, Doha, Qatar

with molecular solvents (Figures 1c and 1d); the three central sub-sections focus on ILs at the IL/air, IL/liquid or IL/solid interface, respectively (Figures 1e-1g); the three final sub-sections analyze the behavior of IL thin films stabilized between two boundaries: air/solid, air/liquid, solid/solid (Figures 1g-1i), respectively.

Experimental

Molecular dynamics (MD) of condensed phases of different pure ILs, molecular solvents (water) and solid substrates (silica, alumina, mica) were carried out using the DLPOLY package.[8] All IL molecular ions were modeled using a previously described all-atom non-polarizable force field (CL&P),[9-14] which is based on the optimized potentials for liquid simulations, all atom (OPLS-AA) framework[15] and specifically developed to encompass entire IL homologous series. OPLS-AA parameterizations were employed for the other species. Some of the MD trajectories used in this work originated from previous works on the same or similar systems.[16-21] Nevertheless, all discussions are based on new analyses performed on new or prolonged MD runs.

When studying nanostructured fluids, the size of the systems and the duration of the simulations are of particular importance since periodic boundary conditions can induce artificial finite-size effects on the length scales of the observed nanostructures. Most system sizes were chosen as to contain at least 13,000 atoms, which correspond to cutoff distances above 1.6 nm. Due to the slow dynamics of IL systems, special care was taken to ensure the attainment of equilibrium conditions: (*i*) equilibrations started from

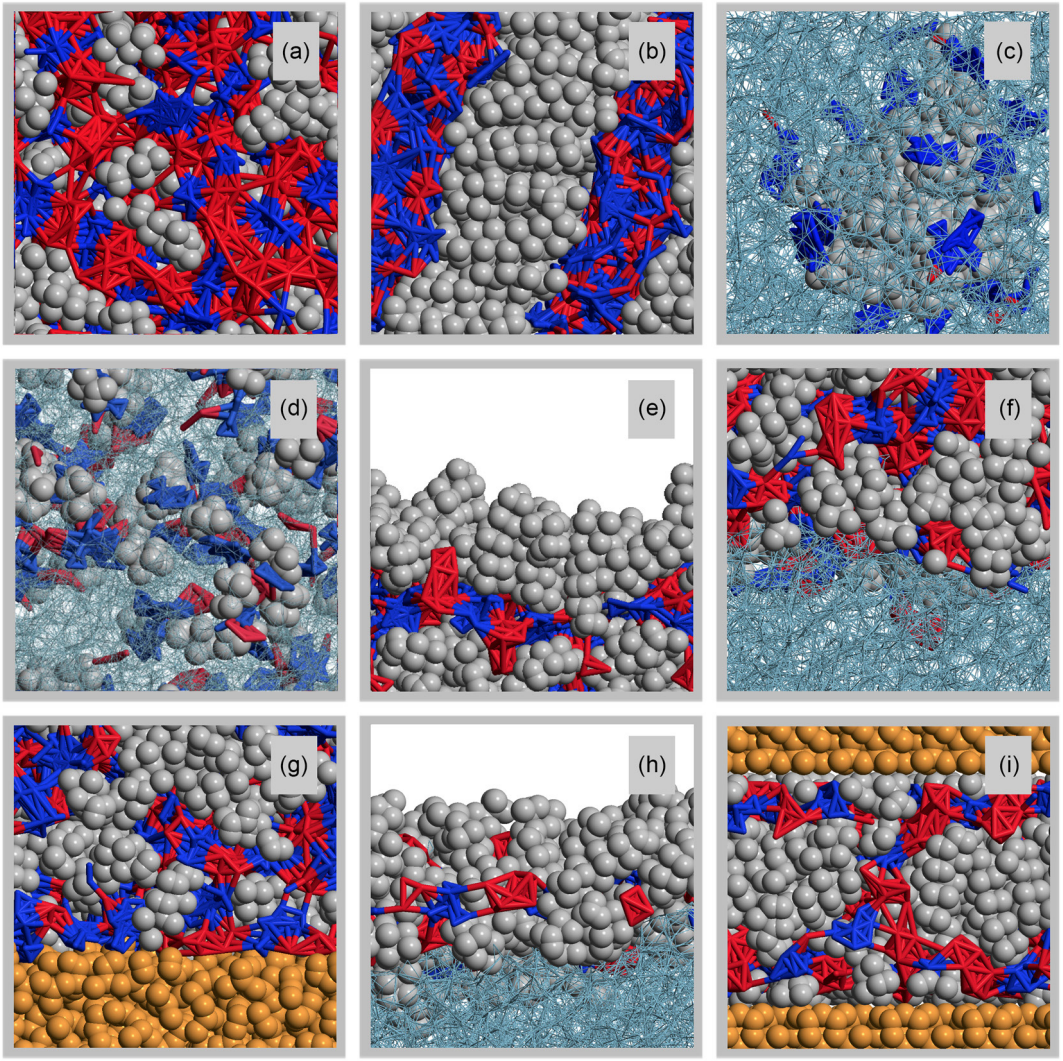

Figure 1. Simulation snapshots depicting different types of structural/boundary features discussed in this work. All images have been represented in the same scale, the side of each square measuring 3.5 nm. The polar moieties of the IL are represented as a blue and red mesh (cations and anions, respectively), the non-polar alkyl side chains of the cations as grey space-filled atoms, water molecules as a turquoise mesh, air/vacuum phases as a white background and solid substrates (mica, alumina) as space-filled atoms. Details concerning the nature of the different ILs are given in each subsection.

initial low-density configurations, with ions placed at random in periodic cubic boxes; (*ii*) typical equilibrations were implemented for more than 1 ns under isothermal-isobaric (N-p-T) ensemble conditions (under the action of Nosé-Hoover barostat and thermostat); (*iii*) multiple re-equilibrations through the use of temperature annealing and switching off and on of the Coulomb interactions were performed; (*iv*) further simulation runs were used to produce equilibrated systems at the studied temperatures. The equilibrated systems were used in production runs of at least 4 ns. Electrostatic and repulsive-dispersive interactions were explicitly calculated for distances below the 1.6 nm cutoff. In the case of repulsive-dispersive interactions, long-range corrections were applied assuming the system had a uniform density beyond this cutoff radius. Long-range electrostatic interactions were treated using the Ewald summation method considering six reciprocal-space vectors. Special boundary conditions/corrections were applied to systems with slab geometries (explicit interfaces).

Structural analyses involved the calculation of radial, cylindrical and spatial pair distribution functions (RDFs, CDFs and SDFs, respectively), structure factor functions (S(q)) and aggregation analyses based on five especially defined statistical tools that allow the estimation of (*i*) average aggregation numbers; (*ii*) and (*iii*) number of contact neighbors in average and within a given aggregate, respectively; (*iv*) aggregate length and (*v*) aggregate volume.

Complementary experimental results were obtained via different methods, ranging from diffraction, microscopy and spectroscopy techniques (small and wide-angle X-ray scattering-SWAXS, atomic force microscopy-AFM) to the determination of thermophysical properties (densimetry, calorimetry, tensiometry, solubility).[22-34]

Results and Discussion

Pure ILs in the bulk phase

The notion that the structure of ILs is complex and can exhibit nanoscale segregation started to be investigated almost ten years ago via molecular modeling studies,[35-37] with the pioneering study in this area performed in Brazil by Urahata and Ribeiro.[35] The existence of mesoscopic structures composed by different moieties of the molecular ions of ILs was confirmed experimentally in 2007 by X-ray diffraction[33] and the interpretation of the corresponding spectra has been an area of intense debate since then.[26,38-41] Experimental evidence linking the structure of ILs to their macroscopic properties has also been interpreted in terms of the underlying nanoscale segregation.[42,43]

The nano-structuration in pure ILs in the bulk phase can be summarized as the superimposition of two types of ordering of the liquid phase with two distinct characteristic wavelengths: (*i*) the ionic character of the fluid imposes some sort of charge ordering which induces the development of a polar network formed by ions of alternating sign —the first contact shell of a given ion is always composed by its counter-ions, Figure 2b; (*ii*) the existence in many ILs of non-polar moieties associated to the molecular ions (generally alkyl side chains) causes the segregation between the polar network and non-polar domains. When the volume occupied by the alkyl chains is large enough, those non-polar domains form a second continuous sub-phase, Figure 2c. The structure factor function of a given IL will exhibit charge-ordering peaks (COPs) and polar-non-polar peaks (PNPPs) that correspond to these two types of structuration, Figure 2d.

The preferred solvation of different molecular solutes in different regions of the IL (within the polar network, in the non-polar domains, or even at the interface between the polar and non-polar regions) is one of the most interesting and useful outcomes of the nano-segregated nature of ILs in the bulk liquid phase.[44]

Another possible outcome arises when the size of the non-polar moieties and the nature of the polar network allow the formation of a liquid-crystal phase. Figure 3a shows a MD simulation snapshot of the liquid crystalline structure of 1-dodecyl-3-methylimidzoliun tetrafluoroborate, $[C_{12}C_1im][BF_4]$, an IL that exhibits a smectic phase between 318 and 358 K. Order is still maintained in the direction normal to the planes/strata but disrupted in the two in-plane directions. The corresponding g(r) functions shown in Figures 3b and 3c depict, on one hand, the existence of a 2D network of alternating ions within each polar layer and, on the other hand, the organization of the dodecyl chains in non-polar strata where chains originating from two different polar layers adopt interdigitated configurations relative to each other.

Self-aggregation in IL solutions

Given the propensity of a pure IL to structure itself in different types of ordered domains, the ensuing question is what happens if an IL is mixed with a molecular solvent? The answer depends, of course, on the mutual solubility of the components and their relative amounts in the mixture.

Diluted aqueous solutions of ILs containing ions with long alkyl side chains (typically larger than octyl chains) can exhibit self-aggregation phenomena[45,46] similar to that of conventional surfactants, Figure 4a.[25,47-49] In these cases some of the unique properties of ILs, such as their low

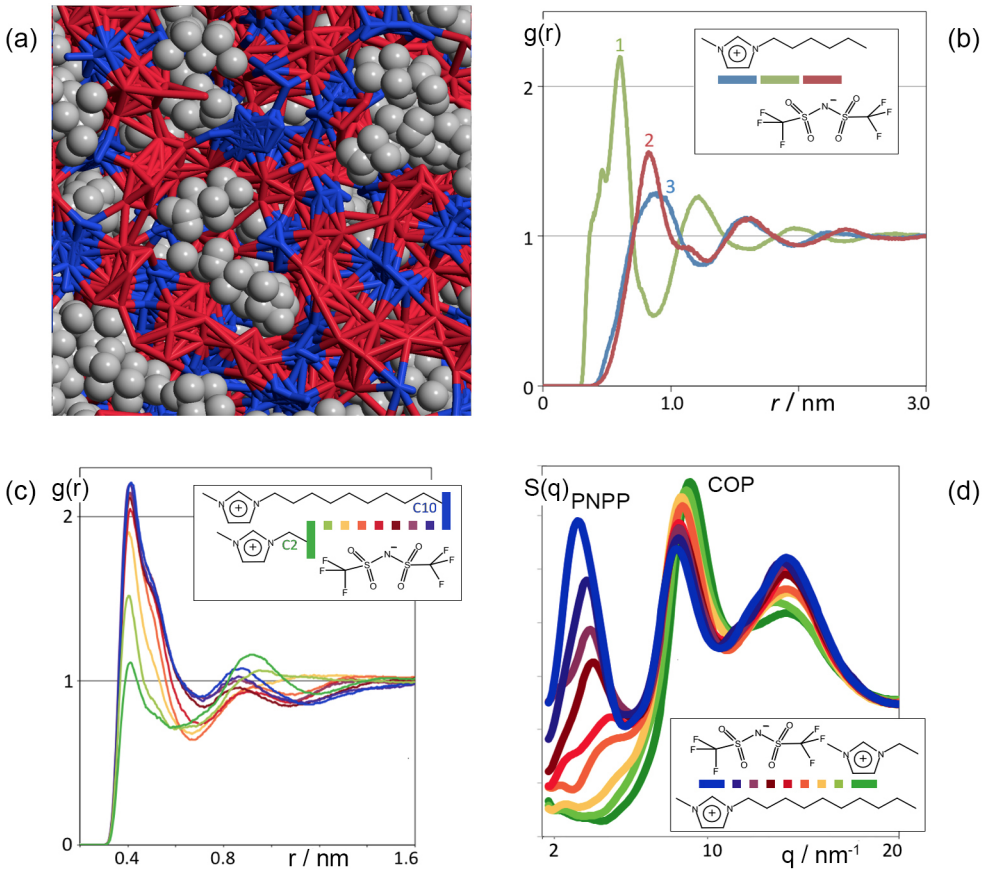

Figure 2. Dual structuration of a pure IL in the bulk phase. (a) MD simulation snapshot of 1-hexyl-3-methylimidazolium *bis*-(trifluoromethylsulfonyl) imide, $[C_6C_1im][Ntf_2]$; (b) pair radial distribution functions, g(r), between selected interaction centers belonging to the charged parts of the $[C_6C_1im]^+$ and $[Ntf_2]^-$ ions. Curve 1: g(r) between the centroid of the imidazolium ring (im) and the nitrogen atom of the anion (NBT); 2: NBT-NBT g(r); 3: im-im g(r). The oscillatory and out-of-phase behavior of the different g(r) functions proves the existence of a polar network in the liquid; (c) g(r)s between the terminal carbon atoms of the alkyl side chains of the cations in the $[C_nC_1im][Ntf_2]$ series ($2 \leq n \leq 10$). The first peak trend (constant above $[C_6C_1im][Ntf_2]$) emphasizes the emergence of a continuous non-polar domain in the liquid; (d) structure factors, S(q), in the same series, depicting the COP and the development of the PNPP.

melting point or their rather sophisticated solvency effects, become minor or of no consequence.[50]

In this context, isothermal titration calorimetry (ITC), a powerful technique for the quantitative investigation of the aggregation properties of surfactants, was used to study the temperature dependent aggregation behavior of three dilalkylpryrrolidinium bromide ILs in aqueous solutions namely: *N*-methyl-*N*-dodecylpyrrolidinium bromide, $[C_1C_{12}Pyrr]Br$, *N*-butyl-*N*-dodecylpyrrolidinium bromide, $[C_4C_{12}Pyrr]Br$, and *N*-butyl-*N*-octylpyrrolidinium bromide, $[C_4C_8Pyrr]Br$. These systems are structurally very close to tetra-alkylammonium salts that are used as traditional ionic surfactants and the similarities or differences to be encountered can contribute to elucidate the mechanisms and the structures responsible for the aggregation of ILs in aqueous solutions, namely micelle formation.

The values of critical micelle concentration, CMC, and micellization enthalpy, $\Delta_{mic}H$, determined at different temperatures using ITC (Figure 4b) of the above mentioned ILs allowed the rationalization of the self-aggregation phenomena in those systems and their correlation with the behavior of analogous traditional surfactants.[51] One of the main conclusions was that $[C_nC_1Pyrr]Br$ surfactants act exactly like the corresponding conventional single-chained surfactants, of the *N*-alkyl-*N*,*N*,*N*-trimethylammonium bromide family, C_nTAB, with similar free energies of transfer of one surfactant molecule from the aqueous to the micellar environment. This conclusion could even be extended to surfactants with two long alkyl chains such as the $[C_mC_nPyrr]Br$ ILs and surfactants of the *N*,*N*-dialkyl-*N*,*N*-dimethylammonium bromide family, C_mC_nDAB.

Aqueous solutions of ILs have some unique and important characteristics: on one hand demixing leads to liquid-liquid equilibrium instead of solid precipitation (like in the case of traditional inorganic salts or ionic surfactants); on the other hand, hydrophilic ILs that are totally miscible with water can form electrolyte solutions ranging in concentration from the pure IL to pure water. In this

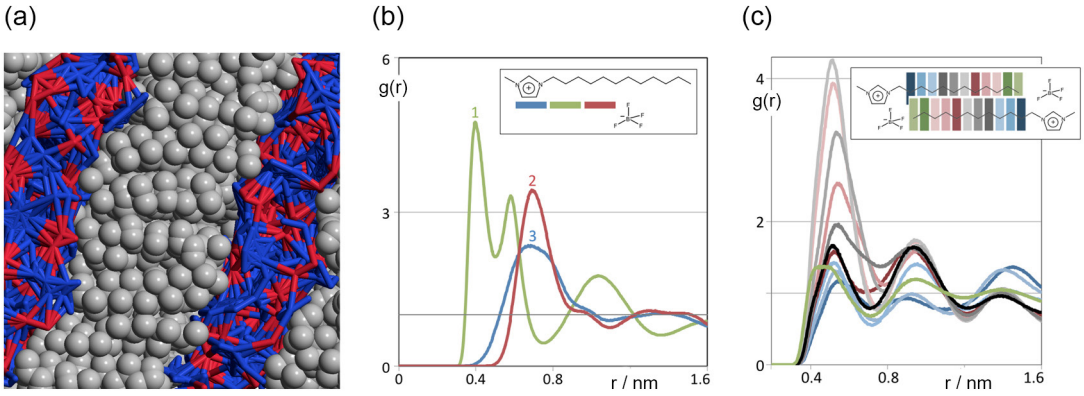

Figure 3. Structuration of a pure IL as a liquid crystalline phase. (a) MD simulation snapshot of 1-dodecyl-3-methylimidazolium tetrafluoroborate, $[C_{12}C_1im][BF_4]$; (b) pair radial distribution functions, g(r), between selected interaction centers belonging to the charged parts of the $[C_{12}C_1im]^+$ and $[BF_4]^-$ ions. Curve 1: g(r) between the centroid of the imidazolium ring (im) and the boron atom of the anion (B); curve 2: B–B g(r); curve 3: im–im g(r). The polar network is present within each polar layer; (c) g(r)s between carbon atoms in the same position of the alkyl side chains of the $[C_{12}C_1im]^+$ ion. The higher g(r) first peaks for the C6 and C7 carbon atoms corroborate the interdigitation of the alkyl chains.

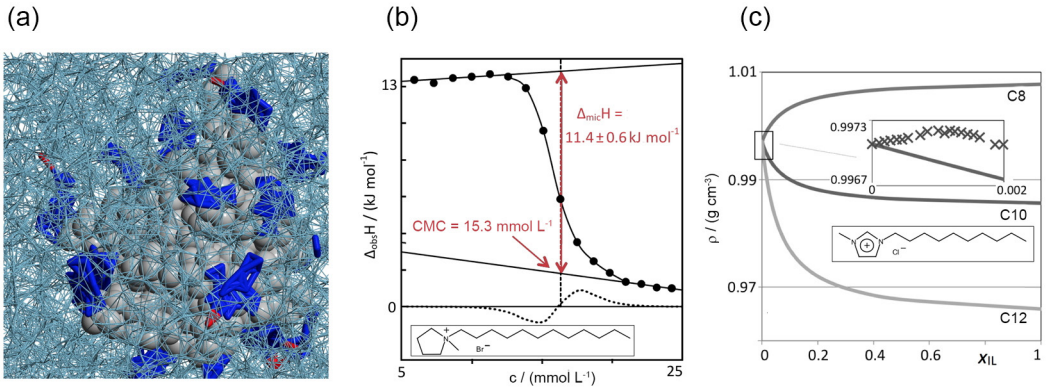

Figure 4. IL micelles in aqueous solution. (a) MD simulation snapshot of a micelle of 1-decyl-3-methylimidazolium chloride, $[C_{10}C_1im]Cl$, in aqueous solution at 298 K; (b) enthalpy change as a function of concentration for the titration of an aqueous solution of *N*-dodecyl-*N*-methylpyrrolidinium bromide, $[C_1C_{12}Pyrr][Br]$, (150 mmol L^{-1}) into water at 323.15 K. The data were fitted in a sigmoidal curve and CMC was obtained as a zero of the second derivative (dotted curve); (c) global ideal volumetric behavior at 298 K of aqueous solutions of $[C_8C_1im]Cl$, $[C_{10}C_1im]Cl$ and $[C_{12}C_1im]Cl$. The inset shows a zoom of the diluted regime comparing the ideal density lines with the experimental density data (x-cross) for $[C_{10}C_1im]Cl$. The position of the CMC can be inferred from the trend shifts in the data.

context we have performed a study on the determination of volumetric data which allows a direct understanding of the relations between the self-aggregation phenomena (micelle formation in this case), the concomitant structural changes that occur in the aqueous solutions and the corresponding consequences at a volumetric level (Figure 4c).

The three ILs selected for such study[24] were members of the 1-alkyl-3-methylimidazolium chloride homologous series-$[C_8C_1im]Cl$, $[C_{10}C_1im]Cl$ and $[C_{12}C_1im]Cl$-and are hydrophilic ILs that form micelles in aqueous solutions at quite distinct concentration ranges, the choice of these ILs also reflected the emphasis given to the measurement of volumetric properties: their specific densities are all very close to that of pure water: at 298 K $[C_8C_1im]Cl$ is slightly more dense than water, whereas the other two are slightly less dense than water. These two sets of properties (different CMCs, similar densities) imposed a rather stringent test to the capability of evaluating micelle formation using volumetric data in the corresponding diluted aqueous solutions.

The global volumetric behavior at 298 K of the three aqueous solutions containing the three ILs under analysis is depicted in Figure 4c, which shows the expected density profiles of each solution if all mixtures exhibited null excess molar volumes (ideal volumetric behavior, i.e., $\rho_{id} = (x_1M_1 + x_2M_2)/(x_1V_1 + x_2V_2)$, with M_i and V_i the molar mass and molar volume of the i^{th} component of the mixture). Figure 4c also shows that, whereas $[C_8C_1im]Cl$ is around 1% more dense than pure water, $[C_{10}C_1im]Cl$ and $[C_{12}C_1im]Cl$ are less dense than pure water by around 1 and 3%, respectively. The inset shows the experimental density data (also at 298 K) for very diluted IL solutions of $[C_{10}C_1im]Cl$ superimposed on the corresponding ideal behavior lines. Some general comments are possible: (*i*) the experimental density data are

always larger than the corresponding ideal values; (*ii*) for the most diluted concentrations, the slopes of the experimental data are almost constant and always larger than the slope of the corresponding ideal lines; (*iii*) at a certain point and for slightly more concentrated solutions, the experimental data slopes start to change and approach the corresponding values (slopes) of the ideal lines. These last trend shifts can be correlated with the attainment of the CMC. For the shown system, the positive deviation between the experimental and ideal values implies that aqueous solutions between 0 and 0.001 mole fraction in the IL exhibit densities that are larger than the densities of both pure water and the pure IL: the density measurements are directly giving a measure of the excess volumetric properties of the mixtures.

The volumetric data show that is indeed possible to estimate the position of the CMC based solely on volumetric data. Moreover, compared to other methods (surface tension, fluorometry, nuclear magnetic resonance) that are frequently used to estimate CMCs, such analysis also provides some insights concerning the behavior of the solute in the midst of the water molecules. The initial increase in the solutions density is caused by the partial break-up of the hydrogen-bonded network of water molecules due to the intrusion of the solute ions, specially the aliphatic moieties that cause the existence of hydrophobic effects. From the CMC region onwards most of the chains will be "hidden" from the water molecules due to micelle formation, which means that the collapse of the water structure will be less pronounced and the density slopes with concentration will become similar.

The last part of this sub-section deals with volumetric measurements performed at more concentrated regimes of similar aqueous solutions (Figure 5).

In case of $[C_8C_1im]Cl$ solutions we have observed gel-like structures in the $0.2 > x_{IL} > 0.4$ concentration range at room temperature. At higher temperatures and IL concentrations, the solutions became clear and fluid again. Figure 5b presents the corresponding volumetric data, expressed as the excess volume of the solutions. The gap in the measurements corresponds to the formation of gel-like systems. For $[C_{10}C_1im]Cl$, the solutions become very viscous (solid-like) above $x_{IL} = 0.06$ concentrations thereby precluding volumetric measurements in the whole composition range. The presence of gel or solid-like phases may indicate the formation of different mesophases in these water-IL systems and is an area currently under investigation.

Another research area where some degree of structuration in bulk aqueous solutions of different ILs occurs is that related to hydrotrope effects. In this case, short-chained hydrophilic ILs such as 1-butyl-3-methylimidazolium dicyanamide, $[C_4C_1im][N(CN)_2]$, are able to increase the solubility of hydrophobic substances in aqueous media by more than one order of magnitude. Although hydrotropes are used to improve the solubility of poorly soluble compounds in water they are not surfactants; the non-polar side chains of hydrotropes are smaller than those of traditional surfactants and they do not form micelles or present a critical micelle concentration (CMC) in the absence of a solute.[47,48] Figure 5a highlights the structure of diluted solutions of $[C_4C_1im][N(CN)_2]$ in water: the continuous polar network that is the hallmark of most pure ILs is broken into smaller aggregates, which nevertheless can still incorporate in some cases a few tens of alternating ions —the size distribution probability functions, $P(n_a)$, of those polar aggregates can be seen in the graph (cat-an) in Figure 5c. In other words, the "dissolved and diluted" IL is not simply a set of isolated

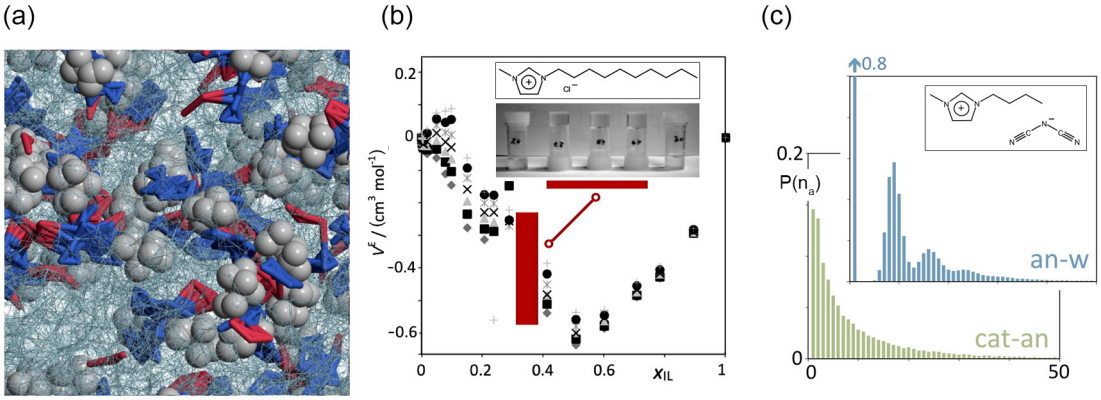

Figure 5. IL strands in aqueous solution. (a) MD simulation of an aqueous solution of 1-butyl-3-methylimidazolium dicyanamide, $[C_4C_1im][N(CN)_2]$ with 0.021 IL mole fraction; (b) volumetric results (excess molar volume data) on aqueous solutions of 1-octyl-3-methylimidazolium chloride, $[C_8C_1im]Cl$, from 283 (rhombs) to 313 K (gray crosses). Concentration ranges from pure water to the pure IL. The vertical rectangle corresponds to concentrations where no density measurements are possible due to the formation of gel-like systems (the up-turned vials correspond to concentrations in the 0.2 to 0.4 IL mole fraction range); (c) discrete probability distribution functions of aggregate sizes, $P(n_a)$, for the broken polar network of 0.021 IL mole fraction solutions of $[C_4C_1im][N(CN)_2]$ in water (cat-an) and for the anion-water network in the same system (an-w).

ions solvated by water molecules, but rather a series of small (and not so small) filamentous ionic strands incorporated within the liquid water matrix. Aggregate analyses of those strands show that the number of neighbors of each ion in a given strand is never much larger than two, which confirms the non-branched and filamentous nature of the aggregates. Moreover, their estimated volume-to-length ratio is generally below 0.03, which means that their shapes can be approximated to elongated prolate ellipsoids. The incorporation of such strands in the aqueous solution can be further probed by the analysis of anion-water aggregates (graph an-w in Figure 5c) that show that the interactive centers of the anions (the nitrogen atoms of dicyanamide) undergo specific H-bond-type interactions with the hydrogen atoms of the water molecules and help to create small networks of alternating water molecules and anions that can contain a few tens of species. It is interesting to note that whereas around 80% of the water molecules do not contact any anion (at the tested concentrations the IL only occupies less than 20% of the total volume of the solution), the remainder 20% of the water molecules becomes part of clusters that are composed of several anions. In fact, the size distribution of the clusters mimics the distribution of the IL clusters present in the solution. In other words, the interactions between the anions and the water molecules help to stabilize those filamentous IL clusters in the midst of the aqueous solution. This complex and unique structure plays an important role in terms of hydrotropy.

The free surface of pure ILs (IL/vacuum interfaces)

The two previous sub-sections dealt with the nano-segregated structure of ILs in bulk phases. The next three sub-sections deal with the rearrangement of those complex structures when they meet a 2D boundary such as the IL/gas, IL/liquid or IL/solid interface. The simpler IL/gas boundary will be considered first (Figure 6).

We start at the free surface of ILs by discussing their surface tension. Among the many unique properties of ILs, their surface tension plays a special role for different reasons. Even at conditions well above room temperature, ILs typically exhibit extremely low vapor pressure values.[52] This fact is a consequence of their ionic nature and makes it difficult to accurately determine the cohesive forces present in the liquid. The use of corresponding states principles and other powerful correlation techniques commonly used for molecular fluids[5] are also difficult to implement. Surface tension values are a way to circumvent an issue that is hard to solve for the bulk fluid but it is possible to access at the liquid-gas boundary —surface tension is a measure of cohesive forces between liquid molecules present at the surface and it represents the quantification of force *per* unit length of free energy *per* unit area. Thus, the measurement of surface tension of ILs is one of the most effective ways to (indirectly) access the intrinsic energetics that are involved in the interactions between the ions. Such measurements are also vital to anchor theoretical models that are able to describe realistically, at a molecular level, the fluid properties and structural nature of ILs.

As we saw, a distinctive characteristic of ILs is their nano-segregated nature. The lack of fluid isotropy already present in the bulk is also present (and sometimes enhanced) at the surface.[53] This means that surface tension data are also a powerful means to explore the different types of segregation/orientation that occur at an ionic/molecular level and how these influence the interactions with other molecules.[54]

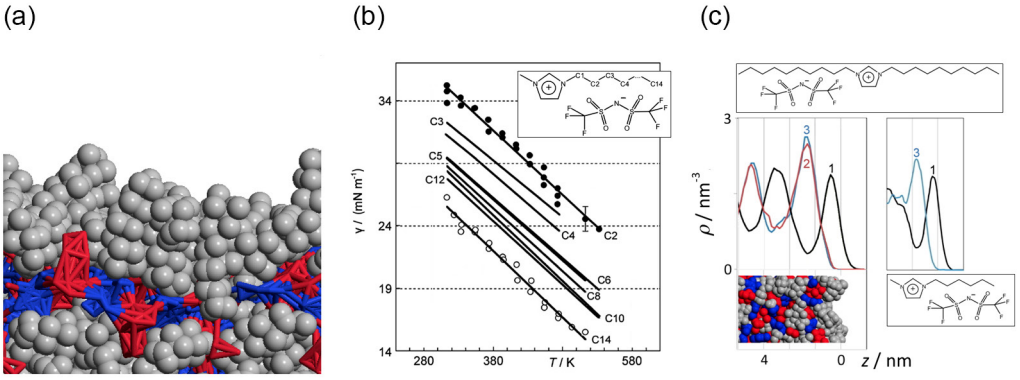

Figure 6. The IL-vacuum interface. (a) MD simulation snapshot of the free surface of 1,3-didecylimidazolium *bis*-(trifluoromethylsulfonyl)imide, $[C_{10}C_{10}im][Ntf_2]$; (b) surface tension as a function of temperature for the $[C_nC_1im][Ntf_2]$ IL series. Experimental points are plotted only for the $[C_2C_1im][Ntf_2]$ and $[C_{14}C_1im][Ntf_2]$ series. The scatter for the other series is similar. The error bar corresponds to the estimated overall uncertainty of the surface tension measurements; (c) numerical density profiles, ρ, along the direction normal to the surface, z, for three selected atom types in $[C_{10}C_{10}im][NTf_2]$: chain terminal carbon atoms (curve 1); nitrogen atom of the anion (curve 2); imidazolium ring centroid (curve 3). The image on the top right shows the same distribution for $[C_6C_1im][Ntf_2]$. The simulation snapshot was scaled and positioned in the same z-scale in order to highlight the free surface. The ions are depicted as red (anions – light gray in the print version), blue (charged parts of the cations – dark gray in the print version), and gray (alkyl side chains) space-filled atoms.

For liquids composed of spherical molecules, e.g., liquid argon or methane, the surface ordering effects are negligible and the surface tension correlates well with the intermolecular interactions in the bulk. In contrast, for liquids composed of non-spherical molecules with polar and non-polar groups, the molecules at the interface may be strongly oriented. According to the Langmuir's principle of independent surface action, each part of a molecule that is actually present at the interface contributes with its own surface free energy to the surface tension of the liquid. In the case of spherical molecules the liquid surface should represent a random truncation of the bulk, in contrast for non-spherical molecules, where the interface is different from the bulk and the surface tension results from the contributions of the groups that form the outer layer of the interface. Langmuir's principle was successfully applied to the surface tension of ILs[55-57] but its application demands the knowledge of the surface tensions of the separated ions and their moieties. Analysis of a large set of experimental values of surface tension of ILs led Kolbeck *et al*.[57] to conclude that the "observed behavior can be explained in a consistent way considering Langmuir's principle, namely that the surface composition is determined by the interplay of cohesive energy and surface orientation". This means for instance that ILs with long alkyl side chains on either the cation or the anion have the surface region dominated by these tails, which are oriented away from the bulk. However, if the alkyl chains are short or functionalized different effects may occur.

On a first set of experimental determinations, we have measured liquid density and surface tension data in temperature ranges up to 473 K and 532 K, respectively, for 1-alkyl-3-methylimidazolium *bis*(trifluoromethylsulfonyl) amide ILs, $[C_nC_1im][Ntf_2]$ with n = 2-10, 12, and 14.[23] The aim was to test the validity of the above-mentioned theories.

Figure 6 shows that the surface tension decreases with increasing temperature and with the increase of the alkyl side chain length along the $[C_nC_1im][Ntf_2]$ family. The decrease is more significant from $[C_2C_1im][Ntf_2]$ to $[C_5C_1im][Ntf_2]$, less so in the $[C_6C_1im][Ntf_2]$ to $[C_{12}C_1im][Ntf_2]$ range, and shows a noticeable drop from $[C_{12}C_1im][Ntf_2]$ to $[C_{14}C_1im][Ntf_2]$. Part of this irregular behavior can be attributed to the overall uncertainty of the data, including the fact that the surface tension is a property sensitive to the presence of small amounts of impurities. Nevertheless one can always speculate that part of the observed trends are a manifestation of different types of arrangements at the surface as the ratio of the non-polar to polar moieties of the ILs is altered by the increase in length of the alkyl side chains. Interestingly this could also be a reflection of what is happening in the bulk phase: MD simulations and X-ray diffraction studies[32,58] have shown that in the case of the $[C_nC_1im][Ntf_2]$ family, there is a transition in the bulk structure of the ILs around $[C_6C_1im][Ntf_2]$ (formation of non-polar continuous domains). It is also known that with alkyl side chains above 12 carbon atoms long there is the possibility of a transition from an isotropic (albeit nano-structured) fluid to a partially layered (more smectic-like) fluid,[59] although in the case of $[C_nC_1im][Ntf_2]$ (n = 12-18) ILs no evidence of liquid crystal formation was ever found.[60]

The $[C_nC_1im][Ntf_2]$ series highlights two important features of ILs in terms of their surface tension: for ILs with small side chains (where the influence of the polar network is dominant and direct at the free surface) the surface tension values at 298 K lie in a range (25-60 mN m^{-1}) which is a no man's land between the idiosyncratic value of water (72 mN m^{-1}) and the values of most molecular solvents (usually below 25 mN m^{-1}); on the other hand, as the alkyl side chains become longer, the surface tension values tend to decrease or become constant.

From the structural point of view, such findings can be easily rationalized taking into account the density profiles along the normal to the surface of the different moieties present in the systems. Figure 6c shows one such profile for the free surface of 1,3-didecylimidazolium *bis*(trifluoromethylsulfonyl)imide, $[C_{10}C_{10}im][Ntf_2]$. As one approaches the surface from the vacuum sides, the first layer to be found is composed of the alkyl side chain(s) of the cation. This is immediately followed by a (polar) layer enriched in the charged parts of the ions that compose the IL (the imidazolium ring and the atoms directly attached to it and the *bis*-triflamide anion). The main difference between the system under discussion with dual and symmetrical alkyl side chains in the cations and previous atomistic simulations of members of the $[C_nC_1im][Ntf_2]$ series (with a single long alkyl side chain),[61] is that in the former example the polar layer is followed by a second well-defined layer enriched in alkyl side chains, whereas in the latter cases such secondary nonpolar layer is almost absent (Figure 6c, image on the right). The numerical density profiles also show that this layering continues to be noticeable (albeit subdued) further away from the free surface (alternation between chain rich and polar-head-rich layers). This kind of situation has been previously observed in coarse-grained simulations of single-chained cations (10 or 12 carbon atoms long chains) combined with small and rigid anions.[62]

ILs at the IL/liquid interface

If the IL/vacuum interface is to be replaced by an IL/liquid interface, than the two liquids must be (at least partially)

immiscible. One of the most studied molecular solvents studied in this context is water, which means that instead of using the hydrophilic ILs given as examples in "self-aggregation in IL solutions", one must switch back to more hydrophobic ILs. Figure 7a exemplifies this with a simulation snapshot of the $[C_{18}mim][Ntf_2]$-water interface. The most striking difference relative to the IL-vacuum interface is that the charged parts of the ions get closer to the interface, instead of the alkyl side chains. The layering patterns already observed for the IL-vacuum interface are also present in this case (Figure 7b), although their intensity and dampening when moving away from the surface is strongly dependent on the size of the alkyl side chains attached to the ions and the nature of the anion. Such structures at the interface between two liquids are particularly difficult to probe experimentally, and several studies derived from the collaboration between experimental and modeling techniques are currently being developed.[63-68]

On the other hand, this type of systems, where liquid-liquid demixing occurs, are particularly important in terms of separation processes. A specially relevant case is the formation of aqueous biphasic systems (ABS) where an IL is mixed with an aqueous solution containing a salting-out agent such as an inorganic salt ($K_3[PO_4]$ is one of the most commonly used), Figure 7c. The name biphasic stems from the fact that when the IL is salted-out from the aqueous solution it usually carries with it a relatively high proportion of water molecules (both hydrophilic and hydrophobic ILs are hygroscopic). The partition of a solute molecule between the two phases of an ABS system must necessarily pass through the "IL-rich"-"water-rich" interface and the modeling described in the previous paragraphs can be an important tool in designing and optimizing such separation processes.[69]

ILs adsorbed at a solid surface

The adsorption of surfactants on solid surfaces has been the subject of numerous studies. This phenomenon has widespread technological applications in wetting, adhesion, nano-fabrication, cleaning and degreasing of metal surfaces. The adsorbed layers (typically of nanometric size) are known to play a key role in the development of new electronic devices, sensor materials and surfaces with special wetting properties. Several attempts have been made to understand the nanoscopic features of the adsorbed layers which are required for the design of interfaces with desired characteristics, such as wetting, agglomeration and friction properties.[70] Particularly relevant are studies related to the self-organization of amphiphilic molecules (anionic, cationic, zwitterionic and mixed micellar systems) and the factors responsible for the alteration of the corresponding structures. The resulting shapes of the adsorbed aggregates are considered to be a compromise between packing effects and specific constraints due to molecule-substrate interactions. The micelles of conventional surfactants adsorbed at the solid-liquid interface are generally considered to be stable only in the presence of the solution —the ordered structure may be lost when the solvent is taken out from the system. However, some cases have been reported, where the regular packing of two-dimensional aggregates formed by amphiphilic molecules at the solid-liquid interface have been successfully preserved at the solid substrate after solvent removal.[71] The behavior of ILs at solid surfaces has been the focus of different works.[17,22,72-74]

Figure 8a shows the IL 1-methyl-3-octylimidazolium tetrafluoroborate adsorbed at an alumina surface.[19] The objective of that work was to clarify the nature of the lamellar

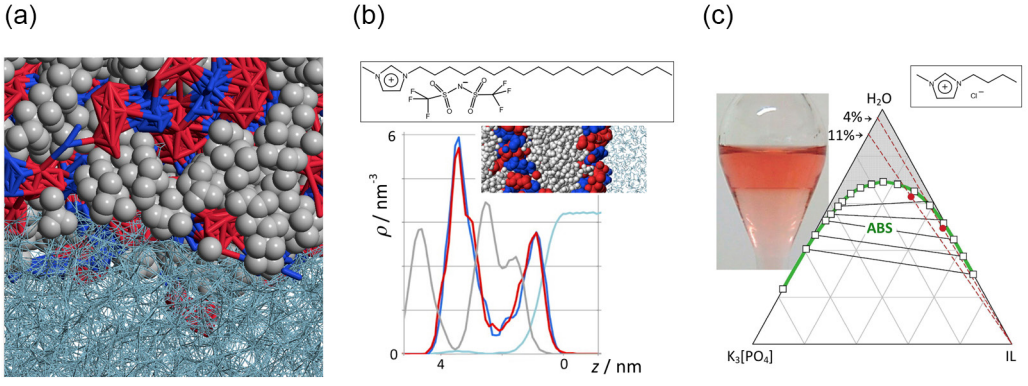

Figure 7. The IL-water interface. (a) MD simulation snapshot of the interface between 1-tetradecyl-3-methylimidazolium *bis*-(trifluoromethylsulfonyl)imide, $[C_{14}C_1im][Ntf_2]$; (b) numerical density profiles, ρ, along the direction normal to the water surface, z, for three selected atom types in $[C_{18}C_1im][Ntf_2]$: chain terminal carbon atoms; nitrogen atom of the anion; imidazolium ring centroid. The image on the top right shows the corresponding simulation snapshot. The ions are depicted as red (anions – light gray large spheres in the print version), blue (charged parts of the cations – dark gray in the print version), and light gray space-filled atoms; (c) ternary diagrams of ($K_3[PO_4]$ + $[C_4mim]Cl$ + H_2O) at 298 K and a nominal pressure of 0.1 MPa. Comparison of our data (circles) with those of Rogers and co-workers (empty squares)[75] in the ABS region.

structure reported by several authors[76-82] for ILs at solid interfaces. The interfacial structure was investigated using atomic force microscopy imaging and MD simulations. It concluded that the behavior of the IL adsorbates is strongly dependent on time and concentration of the IL solution used to deposit the IL at the surface. Structures can vary from liquid-like structures, coexisting liquid and solid phases, and solid-like (ziggurat-type) structures.

On the other hand, a similar study conducted exclusively by MD of 1-(2-hydroxyethyl)-3-methylimidazolium tetrafluoroborate, $[(OH)C_2C_1im][BF_4]$ at the surface of amorphous silica (Figure 8b), concluded that the adsorption and stratification process of ILs over solid substrates can be correctly modeled using a realistic rendition of a non-uniform amorphous substrate such as a glass material and that the stratification occurs even in the absence of long alkyl side chains. The resulting layered structures can be seen as a consequence of the compact and alternate packing of the ions at the solid surface, which is dominated by charge-template effects produced by the amorphous substrate.

Finally, the adsorption behavior of 1-alkyl-3-methylimidazolium chloride ILs on a gold surface was investigated via the measurement of dissipation factors using a quartz crystal microbalance (QCM) and the observation of the morphology and structural patterns formed by diluted IL surfactant solutions dried on the surface. Comparison of the height profile of the $[C_{10}C_1im]Cl$ layer (2-3 nm, Figure 8c) with the hydrodynamic diameter, 1.4 nm[83] for this IL suggests that the uppermost part of this layer reflects the structure of cylindrical micelle structures. We should stress that the AFM images only provide information about the topography of the outer surface and does not allow the estimation of the thickness of all adsorbed layers.

IL Langmuir films at the air/water interface

The knowledge of the structure and packing of ILs at interfaces is of utmost importance for the rational design of such media. A key aspect in the design and preparation of functional materials is the control of intermolecular interactions and molecular packing in the first few monolayers at the surface.[84]

The air-liquid interface is an ideal model surface that is easy to prepare in a pure and well-characterized state and whose surface coverage can be smoothly adjusted using trough techniques. IL Langmuir films are thus extremely important in this context.

The behavior of trihexyl(tetradecyl)phosphonium *bis*(trifluoromethylsulfonyl)imide, $[P_{6\,6\,6\,14}][Ntf_2]$, at the water-air interface was investigated using the Langmuir trough technique (Figure 9a). The obtained surface pressure *versus* mean molecular area (MMA) isotherms, π-A, show distinct regimes (Figure 9b). The results were interpreted at a molecular level using molecular dynamics simulations: the different compression regimes along the $[P_{6\,6\,6\,14}][Ntf_2]$ isotherm correspond to the self-organization of the ions at the water surface into compact and planar monolayers that coalesce at a MMA value of ca. 1.85 nm^2 *per* ion-pair to form an expanded liquid-like layer. Upon further compression the monolayer collapses at around 1.2 nm^2 *per* ion-pair to yield a progressively thicker and less organized

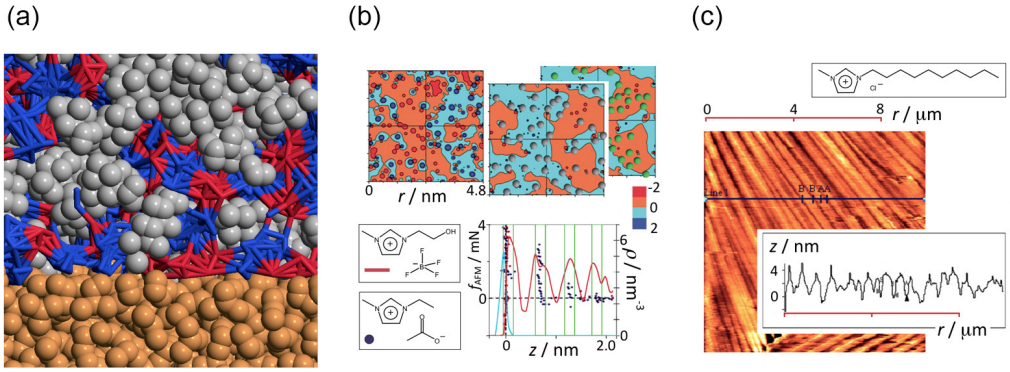

Figure 8. ILs adsorbed on solid substrates. (a) MD simulation snapshot of the interface between 1-methyl-3-octylimidazolium tetrafluoroborate, $[C_8C_1im][BF_4]$, and an alumina, Al_2O_3, amorphous surface; (b) top view of the IL-glass interface of 1-(2-hydroxyethyl)-3-methylimidazolium tetrafluoroborate adsorbed on amorphous silica. The contour graphs in the top row show the electric fields generated by the glass atoms (graph on the left) and the IL ions (two graphs on the right). Selected carbon atoms from the imidazolium ring of the cation (C2, gray spheres) and boron atoms from the anion (green spheres, light gray in the print version) contained in the 0.5 nm thick layer closest to the glass surface are also presented in the two right graphs. The color scale is in electric field units of 1.44×10^{11} J C^{-1} m^{-1}. The bottom graph represents number density profiles of the $[BF_4]^-$ ions (red, right axis – light gray in the print version) and the silanol groups at the glass surface (light blue, right axis – black in the print version) overlaid on top of the force profile of an AFM tip approaching and retracting from a mica surface covered with the $[C_2C_1im][CH_3COO]$ (data points from reference 85, left axis). The vertical lines were drawn around the separation distances between layers given in the same reference. The silanol number density was divided by a factor of three to fit the scale on the right; (c) AFM image of a pure gold substrate treated with an aqueous solution of $[C_{10}C_1im][Cl]$ (0.07 mol L^{-1}), along with the corresponding section analysis.

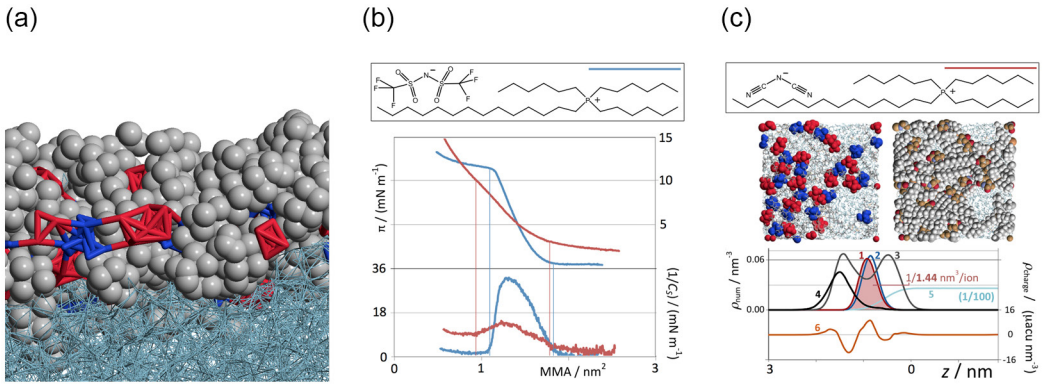

Figure 9. IL Langmuir film at the air/water interface. (a) MD simulation snapshot of a Langmuir film of trihexyl(tetradecyl)phosphonium *bis*(trifluoromethylsulfonyl)imide, $[P_{6\,6\,6\,14}][Ntf_2]$, at the air-water interface; (b) room-temperature isotherms of the $[P_{6\,6\,6\,14}][Ntf_2]$ system at the air water-interface: (top) surface pressure *versus* mean molecular area (MMA) data, π-A; (bottom) compressional modulus, $(1/C_S)$, *versus* MMA data; (c) (top) MD simulation snapshots of the $[P_{6\,6\,6\,14}][Ntf_2]$ systems with a surface MMA value of 1.44 nm^2 *per* ion pair. The left image highlights the positions of the anions (red – light gray space-filled atoms in the print version) and the central charged cores of the cation (blue – dark gray spheres in the print version). The right image uses CPK colors (anions in dark gray and non-polar alkyl chains in light gray space-filled atoms in the print version. Bottom numerical and charge density profiles along the direction normal to the water-vacuum surface. Anion density as curve 1; imidazolium ring densitiy as curve 2; hexyl and tetradecyl terminal carbon atom densitiy as curves 3 and 4, respectively; water molecule density as curve 5. Charge density is represented as curve 6.

layer. The numerical density profiles obtained from the MD simulation trajectories are also able to emphasize the very unusual packing of the four long alkyl side chains of the cation above and below the ionic layer that forms at the water surface (Figure 9c).

IL thin films between solid substrates

ILs containing short alkyl side chains form layered structures at charged surfaces, as seen both from experiments[85-88] and simulations,[89-93] consisting of alternating cation/anion monolayers ("Section: ILs adsorbed at a solid surface"). This layering is also observed in confinement between two extended charged surfaces.[94-99] On the other hand, ILs with long alkyl side chains can self-assemble to form lamellar bilayers in confinement.[97,98] With the ongoing miniaturization of devices, they are prospective lubricants for nano/microelectromechanical systems (NEMS/MEMS), where lubrication must be achieved with films with only a few molecular layers. At such small length scales, surface forces dominate, and it becomes critical to understand molecular friction, adhesion, and wear mechanisms at such scales.

Figure 10a shows a simulation snapshot of the system *N*-decyl-*N*-methylpyrrolidinium *bis*(trifluoromethylsulfonyl)imide, $[C_{10}C_1pyrr][Ntf_2]$, confined between two mica plates a few nanometers apart. The structure of the modeled system is probed via the numerical density profiles depicted in Figures 10b and 10c. The layered structure is emphasized by the presence of the two 2D boundaries and subtle effects such as anion orientation or alkyl side chain interdigitation must take place in order to accommodate all species both from the charge ordering and packing points of view.

These findings are relevant not only to the understanding of lubrication in ILs, but also to the rationalization of

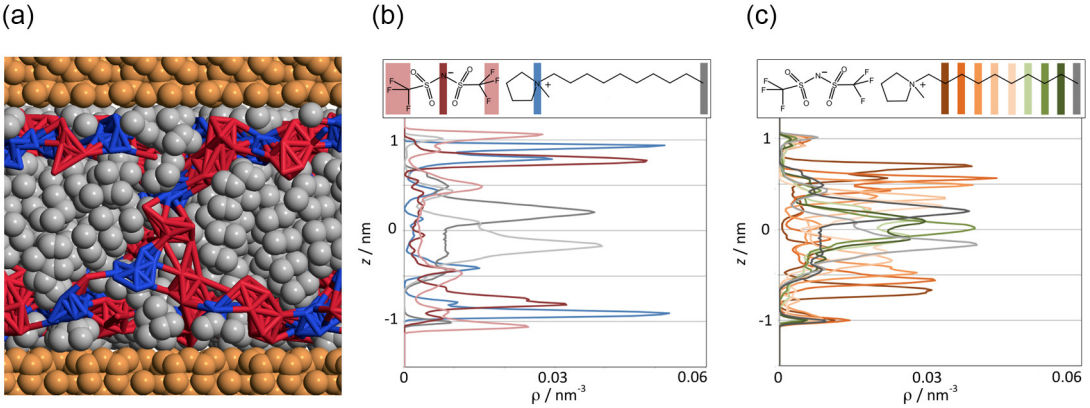

Figure 10. IL film confined between two solid surfaces. (a) MD simulation snapshot of a film of *N*-decyl-*N*-methylpyrrolidinium *bis*(trifluoromethylsulfonyl) imide, $[C_{10}C_1pyrr][Ntf_2]$, confined between two mica plates ca. 2.4 nm apart; (b) and (c) numerical profiles along the direction normal to the mica surfaces. Color codes (grayscale in the print version) given by the different moieties of the molecules in the graph insets.

similar molecular mechanisms that occur in other types of structured phases that we have discussed in the present overview, from liquid crystals to surfactant solutions at high concentration.

Conclusions

Ionic liquids are highly structured fluid media that respond in a quite versatile way to the presence of different types of constraints.

The nano-segregation that already exists in bulk pure ILs between a polar network and non-polar domains is responsible for the unique solvation properties of ILs towards different classes of molecular solutes, or, conversely, the formation of IL micelles or other types of aggregate in aqueous solution.

When a second phase is present, the IL stratifies itself at the 2D interface in order to accommodate its moieties according to the interactions present in the other phase: the non-polar moieties point towards the vacuum phase at the free-surface of an IL; the charged moieties point towards an associative solvent like water or a charged surface like a solid substrate. The nature of the stratification will depend on both the nature of the IL and of the other phase.

Finally, when a molecular-thin film of an ionic liquid is positioned between two interfaces (air-water and solid-solid were given as possible examples), the structuration imposed on the ionic liquid from the dual interface present above and below the film must be taken into account. This leads in some cases to the formation of stable Langmuir films or in other cases to the development of symmetrical arrangements that must match the charge templating and packing effects caused by the system geometry.

All these IL features can be probed and quantified at a molecular level using molecular dynamics simulations and statistical analysis techniques, anchored and validated by relevant experimental data.

Acknowledgements

Financial support provided by Fundação para a Ciência e Tecnologia (FCT) through projects FCT-ANR/CTM-NAN/0135/2012, PTDC/QUI-QUI/117340/2010 and UID/QUI/00100/2013. K. S. and A. A. F. acknowledge the postdoctoral grants SFRH/BPD/94291/2013 and SFRH/BPD/94299/2013, respectively.

References

1. Plechkova, N. V.; Seddon, K. R.; *Chem. Soc. Rev.* **2008**, *37*, 123.
2. Bunton, C. A.; Nome, F.; Quina, F. H.; Romsted, L. S.; *Acc. Chem. Res.* **1991**, *24*, 357.
3. Quina, F. H.; Alonso, E. O.; Farah, J. P. S.; *J. Phys. Chem.* **1995**, *99*, 11708.
4. Freitas, A. A.; Quina, F. H.; Carroll, F. A.; *J. Phys. Chem. B* **1997**, *101*, 7488.
5. Freitas, A. A.; Quina, F. H.; Carroll, F. A.; *Langmuir* **2000**, *16*, 6689.
6. Quina, F. H.; Carroll, F. A.; Cheuy, D. M.; *J. Braz. Chem. Soc.* **2005**, *16*, 1010.
7. Lovelock, K. R. J.; *Phys. Chem. Chem. Phys*. **2012**, *14*, 5071.
8. Smith, W.; Forester, T. R.; *The DL_POLY Package of Molecular Simulation Routines (v.2.2); The Council for The Central Laboratory of Research Councils*; Daresbury Laboratory, Warrington, 2006.
9. Lopes, J. N. C.; Deschamps, J.; Pádua, A. A. H.; *J. Phys. Chem. B* **2004**, *108*, 2038.
10. Lopes, J. N. C.; Pádua, A. A. H.; *J. Phys. Chem. B* **2004**, *108*, 16893.
11. Lopes, J. N. C.; Pádua, A. A. H.; *J. Phys. Chem. B* **2006**, *110*, 19586.
12. Lopes, J. N. C.; Pádua, A. A. H.; Shimizu, K.; *J. Phys. Chem. B* **2008**, *112*, 5039.
13. Shimizu, K.; Almantariotis, D.; Gomes, M. F. C.; Pádua, A. A. H.; Lopes, J. N. C.; *J. Phys. Chem. B* **2010**, *114*, 3592.
14. Lopes, J. N. C.; Pádua, A. A. H.; *Theor. Chem. Acc.* **2012**, *131*, 1129.
15. Jorgensen, W. L.; Maxwell, D. S.; Tirado-Rives, J.; *J. Am. Chem. Soc.* **1996**, *118*, 11225.
16. Shimizu, K.; Bernardes, C. E. S.; Lopes, J. N. C.; *J. Phys. Chem. B* **2014**, *118*, 567.
17. Shimizu, K.; Pensado, A. S.; Malfreyt, P.; Pádua, A. A. H.; Lopes, J. N. C.; *Faraday Discuss.* **2012**, *154*, 155.
18. Cláudio, A. F. M.; Neves, M. C.; Shimizu, K.; Lopes, J. N. C.; Freire, M. G.; Coutinho, J. A. P.; *Green Chem.* **2015**, *17*, 3948.
19. Köhler, R.; Restolho, J.; Krastev, R.; Shimizu, K.; Lopes, J. N. C.; Saramago, B.; *J. Phys. Chem. Lett.* **2011**, *2*, 1551.
20. Almeida, H. F. D.; Freire, M. G.; Fernandes, A. M.; Lopes-da-Silva, J. A.; Morgado, P.; Shimizu, K.; Filipe, E. J. M.; Lopes, J. N. C.; Santos, L. M. N. B. F.; Coutinho, J. A. P.; *Langmuir* **2014**, *30*, 6408.
21. Shimizu, K.; Lopes, J. N. C.; da Silva, A. M. P. S. G.; *Langmuir* **2015**, *31*, 8371.
22. Tariq, M.; Serro, A. P.; Colaço, R.; Saramago, B.; Lopes, J. N. C.; Rebelo, L. P. N.; *Colloids Surf., A* **2011**, *377*, 361.
23. Tariq, M.; Serro, A. P.; Mata, J. L.; Saramago, B.; Esperança, J. M. S. S.; Lopes, J. N. C.; Rebelo, L. P. N.; *Fluid Phase Equilib.* **2010**, *294*, 131.
24. Tariq, M.; Moscoso, F.; Deive, F. J.; Rodriguez, A.; Sanromán, M. A.; Esperança, J. M. S. S.; Lopes, J. N. C.; Rebelo, L. P. N.; *J. Chem. Thermodyn.* **2013**, *59*, 43.

25. Tariq, M.; Podgorsek, A.; Ferguson, J. L.; Lopes, A.; Gomes, M. F. C.; Pádua, A. A. H.; Rebelo, L. P. N.; Lopes, J. N. C.; *J. Colloid Interface Sci*. **2011**, *360*, 606.
26. Hardacre, C.; Holbrey, J. D.; Mullan, C. L.; Youngs, T. G. A.; Bowron, D. T.; *J. Chem. Phys.* **2010**, *133*, 74510.
27. Kashyap, H. K.; Santos, C. S.; Murthy, N. S.; Hettige, J. J.; Kerr, K.; Ramati, S.; Gwon, J.; Gohdo, M.; Lall-Ramnarine, S. I.; Wishart, J. F.; Margulis, C. J.; Castner, E. W.; *J. Phys. Chem. B* **2013**, *117*, 15328.
28. Yamaguchi, T.; Mikawa, K.; Koda, S.; Fujii, K.; Endo, H.; Shibayama, M.; Hamano, H.; Umebayashi, Y.; *J. Chem. Phys.* **2012**, *137*, 104511.
29. Gontrani, L.; Russina, O.; lo Celso, F.; Caminiti, R.; Annat, G.; Triolo, A.; *J. Phys. Chem. B* **2009**, *113*, 9235.
30. Bodo, E.; Gontrani, L.; Caminiti, R.; Plechkova, N. V.; Seddon, K. R.; Triolo, A.; *J. Phys. Chem. B* **2010**, *114*, 16398.
31. Rocha, M. A. A.; Neves, C. M. S. S.; Freire, M. G.; Russina, O.; Triolo, A.; Coutinho, J. A. P.; Santos, L. M. N. B. F.; *J. Phys. Chem. B* **2013**, *117*, 10889.
32. Russina, O.; Triolo, A.; Gontrani, L.; Caminiti, R.; Xiao, D.; Hines Jr, L. G.; Bartsch, R. A.; Quitevis, E. L.; Plechkova, N.; Seddon, K. R.; *J. Phys.: Condens. Matter* **2009**, *21*, 424121.
33. Triolo, A.; Russina, O.; Bleif, H.; di Cola, E.; *J. Phys. Chem. B* **2007**, *111*, 4641.
34. Triolo, A.; Russina, O.; Fazio, B.; Triolo, R.; di Cola, E.; *Chem. Phys. Lett.* **2008**, *457*, 362.
35. Urahata, S. M.; Ribeiro, M. C. C.; *J. Chem. Phys.* **2004**, *120*, 1855.
36. Wang, Y.; Voth, G. A.; *J. Am. Chem. Soc.* **2005**, *127*, 12192.
37. Pádua, A. A. H.; Lopes, J. N. C.; *J. Phys. Chem. B* **2006**, *110*, 3330.
38. Annapureddy, H. V. R.; Kashyap, H. K.; de Biase, P. M.; Margulis, C. J.; *J. Phys. Chem. B* **2010**, *114*, 16838.
39. Bhargava, B. L.; Devane, R.; Klein, M. L.; Balasubramanian, S.; *Soft Matter* **2007**, *3*, 1395.
40. Castner, E. W.; Wishart, J. F.; *J. Chem. Phys.* **2010**, *132*, 120901.
41. Rocha, M. A. A.; Lima, C. F. R. A. C.; Gomes, L. R.; Schröder, B.; Coutinho, J. A. P.; Marrucho, I. M.; Esperança, J. M. S. S.; Rebelo, L. P. N.; Shimizu, K.; Lopes, J. N. C.; Santos, L. M. N. B. F.; *J. Phys. Chem. B* **2011**, *115*, 10919.
42. Hardacre, C.; Holbrey, J. D.; Nieuwenhuyzen, M.; Youngs, T. G. A.; *Acc. Chem. Res.* **2007**, *40*, 1146.
43. Castner, E. W.; Wishart, J. F.; Shirota, H.; *Acc. Chem. Res.* **2007**, *40*, 1217.
44. Freitas, A. A.; Shimizu, K.; Lopes, J. N. C.; *J. Chem. Eng. Data* **2014**, *59*, 3120.
45. Blesic, M.; Marques, M. H.; Plechkova, N. V.; Seddon, K. R.; Rebelo, L. P. N.; Lopes, A.; *Green Chem.* **2007**, *9*, 481.
46. Galgano, P. D.; el Seoud, O. A.; *J. Colloid Interface Sci.* **2010**, *345*, 1.
47. Greaves, T. L.; Drummond, C. J.; *Chem. Rev.* **2008**, *108*, 206.
48. Lee, C. K.; Huang, H. W.; Lin, I. J. B.; *Chem. Commun.* **2000**, *19*, 1911.
49. Ali, M.; Sarkar, A.; Tariq, M.; Ali, A.; Pandey, S.; *Green Chem.* **2007**, *9*, 1252.
50. Angell, C. A.; Byrne, N.; Belieres, J. P.; *Acc. Chem. Res.* **2007**, *40*, 1228.
51. Quina, F. H.; Nassar, P. M.; Bonilha, J. B. S.; Bales, B. L.; *J. Phys. Chem.* **1995**, *99*, 17028.
52. Earle, M. J.; Esperanca, J. M. S. S.; Gilea, M. A.; Lopes, J. N. C.; Rebelo, L. P. N.; Magee, J. W.; Seddon, K. R.; Widegren, J. A.; *Nature* **2006**, *439*, 831.
53. Santos, C. S.; Baldelli, S.; *Chem. Soc. Rev.* **2010**, *39*, 2136.
54. Lockett, V.; Sedev, R.; Harmer, S.; Ralston, J.; Horne, M.; Rodopoulos, T.; *Phys. Chem. Chem. Phys.* **2010**, *12*, 13816.
55. Restolho, J.; Serro, A. P.; Mata, J. L.; Saramago, B.; *J. Chem. Eng. Data* **2009**, *54*, 950.
56. Law, G.; Watson, P. R.; *Langmuir* **2001**, *17*, 6138.
57. Kolbeck, C.; Lehmann, J.; Lovelock, K. R. J.; Cremer, T.; Paape, N.; Wasserscheid, P.; Fröba, A. P.; Maier, F.; Steinrück, H.-P.; *J. Phys. Chem. B* **2010**, *114*, 17025.
58. Pádua, A. A. H.; Gomes, M. F. C.; Lopes, J. N. C.; *Acc. Chem. Res.* **2007**, *40*, 1087.
59. Blesic, M.; Swadzba-Kwasny, M.; Holbrey, J. D.; Lopes, J. N. C.; Seddon, K. R.; Rebelo, L. P. N.; *Phys. Chem. Chem. Phys.* **2009**, *11*, 4260.
60. Hardacre, C.; Holbrey, J. D.; McMath, S. E. J.; Nieuwenhuyzen, M. In *Ionic Liquids-Industrial Applications for Green Chemistry*; Rogers, R. D.; Seddon, K. R., eds.; ACS Symposium Series, American Chemical Society: Washington, DC, USA, 2002, pp. 400-412.
61. Pensado, A. S.; Costa Gomes, M. F.; Lopes, J. N. C.; Malfreyt, P.; Pádua, A. A. H.; *Phys. Chem. Chem. Phys.* **2011**, *13*, 13518.
62. Jiang, W.; Wang, Y.; Yan, T.; Voth, G. A.; *J. Phys. Chem. C* **2008**, *112*, 1132.
63. Wertz, C.; Tschersich, A.; Lehmann, J. K.; Heintz, A.; *J. Mol. Liq.* **2007**, *131-132*, 2.
64. Ahosseini, A.; Sensenich, B.; Weatherley, L. R.; Scurto, A.; *J. Chem. Eng. Data* **2010**, *55*, 1611.
65. Fitchett, B. D.; Rollins, J. B.; Conboy, J. C.; *Langmuir* **2005**, *21*, 12179.
66. Lynden-Bell, R. M.; Kohanoff, J.; del Pópolo, M. G.; *Faraday Discuss.* **2005**, *129*, 57.
67. Chaumont, A.; Schurhammer, R.; Wipff, G.; *J. Phys. Chem. B* **2005**, *109*, 18964.
68. Sieffert, N.; Wipff, G.; *J. Phys. Chem. B* **2007**, *111*, 4951.
69. Freire, M. G.; Claúdio, A. F. M.; Araújo, J. M. M.; Coutinho, J. A. P.; Marrucho, I. M.; Canongia Lopes, J. N.; Rebelo, L. P. N.; *Chem. Soc. Rev.* **2012**, *41*, 4966.
70. Paria, S.; Khilar, K. C.; *Adv. Colloid Interface Sci.* **2004**, *110*, 75.
71. Atkin, R.; Craig, V. S. J.; Biggs, S.; *Langmuir* **2000**, *16*, 9374.

72. Bovio, S.; Podestà, A.; Lenardi, C.; Milani, P.; *J. Phys. Chem. B* **2009**, *113*, 6600.
73. Atkin, R.; el Abedin, S. Z.; Hayes, R.; Gasparotto, L. H. S.; Borisenko, N.; Enders, F.; *J. Phys. Chem. C* **2009**, *113*, 13266.
74. Bovio, S.; Podestà, A.; Milani, P.; Ballone, P.; del Pópolo, M. G.; *J. Phys.: Condens. Matter* **2009**, *21*, 424118.
75. Gutowski, K. E.; Broker, G. A.; Willauer, H. D.; Huddleston, J. G.; Swatloski, R. P.; Holbrey, J. D.; Rogers, R. D.; *J. Am. Chem. Soc.* **2003**, *125*, 6632.
76. Rollins, J. B.; Fitchett, B. D.; Conboy, J. C.; *J. Phys. Chem. B* **2007**, *111*, 4990.
77. Mezger, M.; *J. Chem. Phys.* **2009**, *131*, 094701.
78. Hayes, R.; Warr, G. G.; Atkin, R.; *Phys. Chem. Chem. Phys.* **2010**, *12*, 1709.
79. Liu, Y.; Zhang, Y.; Wu, G.; Hu, J.; *J. Am. Chem. Soc.* **2006**, *128*, 7456.
80. Yokota, Y.; Harada, T.; Fukui, K.; *Chem. Commun.* **2010**, *46*, 8627.
81. Wang, S.; Li, S.; Cao, Z.; Yan, T.; *J. Phys. Chem. C* **2010**, *114*, 990.
82. Sha, M.; Wu, G.; Dou, Q.; Tang, Z.; Fang, H.; *Langmuir* **2010**, *26*, 12667.
83. Bai, G.; Lopes, A.; Bastos, M.; *J. Chem. Thermodyn.* **2008**, *40*, 1509.
84. Dong, B.; Li, N.; Zheng, L.; Yu, L.; Inoue, T.; *Langmuir* **2007**, *23*, 4178.
85. Atkin, R.; Warr, G. G.; *J. Phys. Chem. C* **2007**, *111*, 5162.
86. Mezger, M.; Schroder, H.; Reichert, H.; Schramm, S.; Okasinski, J. S.; Schoder, S.; Honkimaki, V.; Deutsch, M.; Ocko, B. M.; Ralston, J.; Rohwerder, M.; Stratmann, M.; Dosch, H.; *Science* **2008**, *322*, 424.
87. Hayes, R.; el Abedin, S. Z.; Atkin, R.; *J. Phys. Chem. B* **2009**, *113*, 7049.
88. Zhang, X.; Zhong, Y.-X.; Yan, J.-W.; Su, Y.-Z.; Zhang, M.; Mao, B.-W.; *Chem. Commun.* **2012**, *48*, 582.
89. Reed, S. K.; Lanning, O. J.; Madden, P. A.; *J. Chem. Phys.* **2007**, *126*, 084704.
90. Fedorov, M. V.; Kornyshev, A. A.; *J. Phys. Chem. B* **2008**, *112*, 11868.
91. Lynden-Bell, R. M.; Frolov, A. I.; Fedorov, M. V.; *Phys. Chem. Chem. Phys.* **2012**, *14*, 2693.
92. Merlet, C.; Rotenberg, B.; Madden, P. A.; Salanne, M.; *Phys. Chem. Chem. Phys.* **2013**, *15*, 15781.
93. Fedorov, M. V.; Kornyshev, A. A.; *Chem. Rev.* **2014**, *114*, 2978.
94. Perkin, S.; Albrecht, T.; Klein, J.; *Phys. Chem. Chem. Phys.* **2010**, *12*, 1243.
95. Ueno, K.; Kasuya, M.; Watanabe, M.; Mizukami, M.; Kurihara, K.; *Phys. Chem. Chem. Phys.* **2010**, *12*, 4066.
96. Bou-Malham, I.; Bureau, L.; *Soft Matter* **2010**, *6*, 4062.
97. Perkin, S.; Crowhurst, L.; Niedermeyer, H.; Welton, T.; Smith, A. M.; Gosvami, N. N.; *Chem. Commun.* **2011**, *47*, 6572.
98. Smith, A. M.; Lovelock, K. R. J.; Gosvami, N. N.; Licence, P.; Dolan, A.; Welton, T.; Perkin, S.; *J. Phys. Chem. Lett.* **2013**, *4*, 378.
99. Espinosa-Marzal, R. M.; Arcifa, A.; Rossi, A.; Spencer, N. D.; *J. Phys. Chem. C* **2014**, *118*, 6491.

Submitted: August 5, 2015
Published online: October 21, 2015